The current-induced critical field of a type II superconducting cylindrical filament

M. Masale*

Department of Physics, University of Botswana, Private Bag 0022, Gaborone, Botswana

Received 29 November 2000; received in revised form 8 October 2001; accepted 9 October 2001

Abstract

The azimuthal surface nucleation field of an infinitely long type II superconducting cylindrical filament is calculated from the linearized Ginzburg–Landau equation for the order parameter. A current is thought to be passed along the axis of the filament which induces a magnetic field in the azimuthal direction. On increasing the current, the field increases to a value whereby a phase transition from the superconducting to the normal state occurs. The magnetic field lines are parallel to the surface of the cylindrical filament so that the required critical field is H_{c3}; the parallel surface nucleation field of a type II superconductor. The systems considered are a solid cylinder; free-standing and in a metallic matrix; and a very thin-walled hollow cylinder. The full numerical analysis is carried out only for a solid cylinder. In the case of a thin-walled cylindrical shell, the quantitative description of the superconducting–normal phase is given in terms of the limiting form of the temperature for small fields.

PACS: 74.60.Ec
Keywords: Type II superconductor; Cylindrical filament; Current-induced magnetic field

1. Introduction

It has long been known that superconductivity can be destroyed by an applied magnetic field [1]. The flux associated with the applied magnetic field is expelled from the bulk of a type II superconductor for fields less than the bulk critical value, H_{c2} [2]. At this value of the applied field, a type II superconductor undergoes a second order transition from the superconducting to the normal state. Clearly, for fields higher than H_{c2} the flux penetrates the material which is then in the normal state. A higher surface nucleation field, $H_{c3} = 1.69H_{c2}$, appears at the planar surface of a type II superconductor in a parallel magnetic field [3]. In their extensive investigations, both experimental and theoretical, Guyon et al. [4] found that the surface nucleation field of a very thin film is very different from that of either a thick film or a semi-infinite specimen. One of the findings from their investigations was that at a certain critical thickness of the film, it becomes possible for a vortex to fit inside the film. This phenomenon, characterized by a point of inflection on the temperature–field curve, is associated with the first flux-entry point. Motivated by how the parallel surface nucleation

* Tel.: +267-355-2940; fax: +267-585-097.
E-mail address: masalem@mopipi.ub.bw (M. Masale).

field changes according to either the dimensionality or the shape of a superconductor as well as by the advancement in fabrication techniques [5], Masale et al. [6] reconsidered a number of systems with cylindrical symmetry. Distinct flux-entry points, which are quantized in integral multiples of the flux quantum, $\phi_0 = h/2e$, are clearly seen in the universal field–temperature curve of a cylinder in a parallel magnetic field [6–8]. As such, in a very thin-walled hollow cylinder immersed in a parallel magnetic field, the flux-entry points are such a prominent feature of the field–temperature curve giving rise to what are known as Little–Parks oscillations [9]. In the numerous investigations concerned with the critical fields of type II superconducting specimen, the Ginzburg–Landau (G–L) equation has been employed in its linearized form [3,4,6–8]. This is on account of the well known feature of the Landau theory of phase transitions, namely that near a phase transition the order parameter becomes very small [10]. The higher-order terms of the order parameter in the G–L equation may therefore be neglected, giving rise to the linearized form of the G–L equation [8]. This approach provides a scheme of solvable equations which give an adequate quantitative description of total flux exclusion in type II superconducting specimen [4,6,8]. Because of persistent circulating currents at the surface of a superconducting cylinder in a parallel applied magnetic field [11] between H_{c2} and H_{c3}, a long macroscopic superconducting cylinder appears as a giant single vortex [12]. In addition, it has been shown experimentally that a current-carrying state can occur for applied fields less than the bulk critical value, H_{c2} [13].

The aim of this study is to map out the critical field versus temperature curves of type II superconducting cylindrical filaments in the case of a magnetic field applied in the azimuthal direction. The thought experimental set-up is as follows: a current along the axis of a superconducting cylinder induces a magnetic field in the azimuthal direction. The magnetic field lines are parallel to the surface of the superconducting filament. With increasing current, the magnetic field reaches a value of $H_{c3}(\phi)$, the azimuthal parallel nucleation field, at which the cylindrical filament is brought into the normal state. Carrying out indirect resistivity measurements, for example, as in recent experiments on high-T_c superconductors [14], the known critical current can be used in the computation of the required critical field. One of the complications that arises in the systems considered here is that the applied magnetic field is not uniform but instead varies with the radial distance. This raises the question concerning the nature of the trajectories of a charged particle in an inhomogeneous magnetic field and therefore the dependence of the cyclotron frequency on the magnetic field or on the radial distance. A possible consequence of the inhomogeneity of the induced field is that there could arise spatial distributions of the superconducting phases of the specimen. This puts in doubt the adequacy of the linearized G–L equation to provide a realistic account of the superconducting phases across a sample subjected to a spatially inhomogeneous magnetic field. Fink and Presson [12] addressed this question in their analysis of the vortex state based on the full G–L equation, including a discussion on the hysteric nature of the magnetization and its characterization in terms of the relevant Ginzburg parameters. There is a remarkable similarity between the problem formulated by Fink and Presson [12] and the one considered here. The above mentioned similarity arises from the reciprocal nature of a magnetic field and a current to in turn induce one another. The giant vortex state considered [12] comes into existence as a result of the application of a uniform magnetic field parallel to the axis of a solid cylinder. The applied magnetic field induces circulating currents, which are in fact responsible for the Meissner and the mixed states of a type II superconductor, with the result that the cylinder then takes the form of a giant current vortex [11]. Here, the situation is the other way around in that a thought-uniform current density along the cylinder axis generates a spatially inhomogeneous magnetic field in the azimuthal direction. While conventional experiments provide information on the onset of superconductivity [15,16], the above mentioned spatial variations of the superconducting phases should easily be accessible in the newly developed micro-magnetization measurement technique [17].

The lay-out of this paper is as follows: the formalism for the calculation of the azimuthal critical field is outlined in Section 2. The discussion of a solid cylinder, free-standing and in a non-superconducting metallic matrix, is presented in Section 3. Section 4 deals with the system of a thin-walled current-carrying cylindrical shell. A geometrically similar system, that of a cylindrical shell enveloping a current-carrying core, is briefly discussed in Section 5. Finally, the concluding remarks are given in Section 5.

2. Formalism

The superconducting phase of a type II superconductor may be adequately described by the linearized G–L equation for the order parameter ψ given by [10]

$$\frac{1}{2\mu}(-\imath\hbar\nabla - 2e\mathbf{A})^2\psi + \alpha\psi = 0, \tag{1}$$

where $\mathbf{A}$ is the vector potential, μ is the mass of a particle of charge $2e$ and, $\alpha = \alpha_0(T - T_{cb})$, the G–L parameter in terms of the bulk critical temperature T_{cb}. The general expression for the quantum mechanical current density is given by

$$\mathbf{J} = -(\imath e\hbar/\mu)(\psi^*\nabla\psi - \psi\nabla\psi^*) - (4e^2/\mu)|\psi|^2\mathbf{A}. \tag{2}$$

The geometry of the superconductor enters the eigenvalue problem via the boundary condition for a superconductor–insulator interface [15,18],

$$\hat{\mathbf{n}}\cdot(-\imath\hbar\nabla - 2eA)\psi = 0, \tag{3}$$

in which $\hat{\mathbf{n}}$ is a unit vector normal to the interface. For reasons of symmetry, $\mathbf{A} = (0, 0, A_z)$. The solution of the linearized equation for the order parameter is sought in the general form:

$$\psi = C_{m\ell}\exp(ik_z z)\exp(im\phi)\chi(\rho), \quad m = 0, \pm1, \pm2, \ldots, \tag{4}$$

where $C_{m\ell}$ is a constant, k_z is the axial wave number and m is the azimuthal quantum number. With the form of the wave function given by Eq. (4), the G–L equation for the order parameter takes the following form:

$$\rho\frac{\mathrm{d}}{\mathrm{d}\rho}\left(\rho\frac{\mathrm{d}\chi}{\mathrm{d}\rho}\right) - \left[m^2 - 2\frac{\mu}{\hbar^2}|\alpha|\rho^2 + \left(k_z + 2\frac{e}{\hbar}A_z\right)^2\rho^2\right]\chi = 0. \tag{5}$$

Eq. (5), taken together with the form of the boundary condition prescribed by Eq. (3) is employed in the determination of the azimuthal surface nucleation field for the different systems in the following sections. Here, unlike in the case of an axial applied magnetic field [6–8], the required critical field corresponds strictly to the zero angular momentum ($m = 0$) eigenfunction.

3. Current-carrying solid cylinder

The vector potential of the magnetic field due to a uniform current density, $J_{ext} = I/(\pi R^2)$, where I is the current fed into one end of the solid cylinder is taken in the gauge:

$$A_z = -\frac{1}{4}\mu_0 J_{ext}\rho^2, \tag{6}$$

where μ_0 is the permeability of the non-magnetic material. With the explicit form of the vector potential given above, the G–L equation for ψ becomes

$$x\frac{\mathrm{d}^2\chi}{\mathrm{d}x^2} + \frac{\mathrm{d}\chi}{\mathrm{d}x} + \left[\epsilon - \left(\frac{1}{2}k_z R - fx\right)^2\right]\chi = 0, \tag{7}$$

where $x = \rho^2/R^2$, and the temperature ϵ and the field f are defined by the dimensionless variables:

$$\epsilon = \mu|\alpha|R^2/2\hbar^2 \quad \text{and} \quad f = \pi B_s R^2/2\phi_0. \tag{8}$$

Here, $B_s = \mu_0 I/(2\pi R)$, is the value of the magnetic field at the surface of the cylinder. The point about the non-uniformity of the induced magnetic field here needs to be emphasized. The general definition of f may be taken simply as the magnetic flux penetrating a surface perpendicular to the plane of the cyclotron orbit per twice the flux quantum. The difficulty that arises in this case is that not only is the magnetic field inhomogeneous but that the cyclotron orbits are in the plane of the cylinder axis. Eq. (7) is solved numerically since it is not possible to cast it into a canonical form. This

makes it essential, therefore, to develop some limiting forms of its solutions which will serve as a guide to the full numerical solution. For a very small current, the term parabolic in f in Eq. (7) can be neglected and the limiting form of the differential equation that arises is solvable in terms of the confluent hypergeometric function. The solution of the radial equation, W in place of χ, is obtained as:

$$W = \exp(-\varsigma/2)M(a,1,\varsigma), \tag{9}$$

where the parameter a and the argument ς of the confluent hypergeometric function M are given by

$$a = \frac{1}{2} + \frac{\eta}{2}\frac{[\epsilon - \frac{1}{4}k_z^2R^2]}{\sqrt{|k_z|Rf}} \quad \text{and} \quad \varsigma = \eta\sqrt{(|k_z|Rf)}x. \tag{10}$$

For very small currents, Eq. (9) can be solved to obtain the required critical values of the temperature and the field.

3.1. Free-standing

An even less numerically taxing approach for generating the field–temperature curve follows from the constant ψ limiting form of ϵ, obtained by integrating the G–L equation across the thickness of a free-standing solid cylinder. The approximate result is given by:

$$\epsilon \sim \tfrac{1}{4}k_z^2R^2 - \tfrac{1}{2}|k_z|Rf + \tfrac{1}{3}f^2. \tag{11}$$

The corresponding result for a solid cylinder in a parallel magnetic field, which is a slight improvement on the result obtained by Constantinou et al. [8], is as follows:

$$\epsilon \sim \tfrac{1}{2}m^2 - |m|f + \tfrac{2}{3}f^2. \tag{12}$$

The analogous result for a thin film of thickness d in a parallel magnetic field is given by

$$\epsilon \sim \tfrac{1}{4}k_y^2d^2 + \tfrac{1}{3}f^2, \tag{13}$$

where k_y (which must be taken as zero for small f) is the wave vector component perpendicular to the magnetic field and parallel to the walls of the film. The similarity between this problem and that of a thin film in a parallel magnetic field is twofold. As stated earlier, the magnetic field lines are parallel to the boundary of the superconductor. The second feature of similarity is that the center of the cyclotron orbit is determined by the value of the wave vector component, k_y or k_z. It needs to be emphasized that, unlike m, which is discrete, these wave numbers are continuous variables.

It is also helpful to derive the explicit expression for the current density since the nature of the superconducting phase across the cylinder thickness may be inferred from it. Since the radial wave function is real and only the z component of the vector potential is considered, only the z component J_z of the current density is non-zero and is given by

$$\frac{J_z}{J_{0z}} = \chi^2(x)[|k_z|R + 2fx], \tag{14}$$

where $J_{0z} = 2e\hbar/(\mu R)$.

Returning to the eigenvalue problem, the strategy employed to obtain the eigenvalues is as follows [8]: first fix f, then search for the value of the fluxoid number, k_zR (k_yd or m), that gives the lowest value of ϵ. Only the minimum value of ϵ has physical significance since it is the one that corresponds to the required critical field. The key feature that emerges in these systems (Eqs. (11)–(13)) is that in the case of the cylinder in an azimuthal magnetic field, the flux-entry points occur for all non-zero magnetic field values. Despite the similar form of Eqs. (11) and (12), $m = 0$ but $k_z \neq 0$ will give the lowest eigenvalue of ϵ for non-zero field, due to the fact that m is a discrete quantity whereas k_z is a continuous variable. Since k_z is a continuous variable, the presence of the azimuthal field, irrespective of its strength, gives rise to the existence of the $k_z > 0$ bound states. The eigenvalues corresponding to $k_z \leqslant 0$ are larger than those for $k_z > 0$ and therefore have no physical significance.

The temperature–field curves of some type II superconducting filaments are shown in Fig. 1. The main result of this study is shown as curve (a) which represents the full numerical solutions of Eq. (7). The dashed curve (b) is the corresponding constant ψ approximation generated from Eq. (11). The full numerical results for a solid cylinder, curve (c), and that of a thin film, curve (d), in uniform parallel magnetic fields are included here

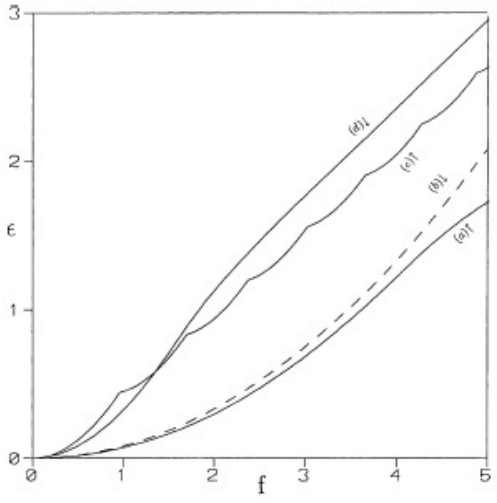

Fig. 1. The critical field–temperature curves for some type II superconducting filaments: (a) solid cylinder in an azimuthal magnetic field, (b) the constant $|\psi|$ approximate result for the system of curve (a), (c) the result for a solid cylinder in a parallel magnetic field and (d) the result for a thin film in a parallel magnetic field.

for reference. First, note the good agreement between the exact, Fig. 1(a), and the approximate results, Fig. 1(b), for the range of the field values assumed here. Second, it is seen that for the given critical temperature, the azimuthal critical field is significantly higher than the parallel critical field of either a solid cylinder or a thin film. This is a direct consequence of having non-zero fluxoid numbers for all the field values in the case of a cylinder in an azimuthal magnetic field. It is worth mentioning that the ϵ–f curve corresponding to $k_z = 0$ follows very closely the critical field–temperature curve of a thin film, at least for the range of the f values assumed. Note also that for very fine filaments (small R or d) all the curves shown in Fig. 1 are parabolic in f. Since for large f (corresponding to a thick cylinder) the curvature of the cylinder can hardly matter, the result for a flat surface in a parallel magnetic field should be recovered. This is not the case here and to this end some few observations are noted as follows: the induced magnetic field is not uniform but increases linearly with the radial distance. This implies that the innermost regions of a thick cylinder, where the field is less than H_{c2}, should be in the superconducting phase. The region just outside the radius R_{c2}, corresponding to the magnetic field contour value of H_{c2}, should then be in the normal state. A superconducting sheath, of course, persists at the surface of the cylinder for fields up to the higher parallel surface nucleation field H_{c3}. Now, with reference to the field–magnetization curve of a type II superconductor [10], the imaginary cylindrical shell of thickness $(R - R_{c2})$ can be in the mixed state, depending on the thickness of the cylinder.

For very thick cylinders the region just outside R_{c2} should be in the normal state. For relatively thin cylinders, when R_{c2} is not very different from R, surface nucleation can in principle extend to the region bounded by R_{c2}. The field just outside this region, however, should still be less than the surface nucleation field.

Fig. 2 shows the radial wave function profiles for some points on the azimuthal critical field–temperature curve of Fig. 1(a). Each curve

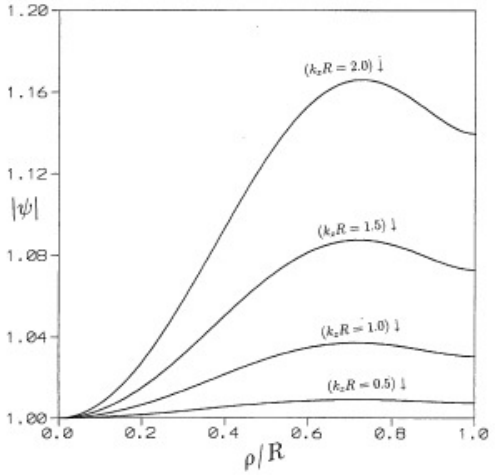

Fig. 2. The wave function profiles across the cylinder for some points on the field–temperature curves shown as Fig. 1(a). In particular, the fluxoid values, indicated against each of the corresponding curves are: $k_zR = 0.5$ for the curve, increasing in steps of 0.5, up to 2.0 for the highest curve.

corresponds to a different value of the fluxoid number. These are: $k_zR = 0.5$, for the lowest curve, increasing in steps of 0.5 up to 2.0 for the highest curve. For small values of f, that is, for $R < \xi$, the radial function can hardly change across the cylinder radius. In the limit of small f, the cylinder nucleates uniformly across its thickness. For intermediate values of the field, $R \sim \xi$, the radial variations of χ begin to emerge. For $\xi > R$, there is a build up of the wave function towards the surface of the cylinder. This confirms the presence of a superconducting sheath near the surface. It is seen from Fig. 2 that for relatively large values of f the radial wave functions are characterized by a peak. The peak occurs near the surface and can therefore extend into the region where the surface nucleation sheath persists. Since the induced magnetic field increases with the increase in the radial distance, this peak may be viewed as signifying the region of the cylinder where, near the surface, the superconducting phase is most stable. Once again, note that the field at the radial distance corresponding to this peak is between H_{c2} and H_{c3}. The fine grid of the χ axis implies that for the used values of k_zR the radial function remains more or less constant across the cylinder thickness. In any case the $\{f, k_zR\}$ points have been selected from the region of the ϵ–f curve where the constant ψ approximation is adequate, compare curves (a) and (b) of Fig. 1. Unlike a cylinder in a uniform parallel magnetic field the radial wave function in this case is finite even at the origin, which implies the presence of superconductivity there. This is confirmed by Fig. 3 for the current density curves corresponding to the wave functions shown in Fig. 2. The curves in Fig. 3 are labelled by their k_zR values, which are: 0.5 for the lowest curve, increasing in steps of 0.5 up to 2.0 for the highest curve. It is seen that J_z builds up towards the cylinder surface for increasing values of k_zR. Again, this is consistent with the persistence of the surface nucleation sheath. The results shown in Figs. 2 and 3 should be regarded as illustrative since they are based on the linearized rather than on the full G–L equation. Furthermore, there can arise an additional superconducting state below H_{c2}. Arguably, an adequate quantitative description of this current-carrying state should be based on the full G–L equation. The results depicted in Figs. 2 and 3 are nonetheless very similar to those obtained from the solutions of the full G–L equation [12]. This suggests that the linearized G–L equation is useful, at least as a first approximation, in the description of the superconducting phases of a sample immersed in a spatially inhomogeneous magnetic field.

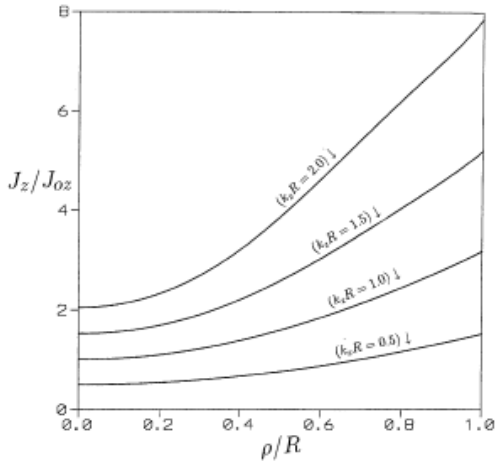

Fig. 3. The distribution of the quantum mechanical current density across the cylinder radius corresponding to the wave functions shown in Fig. 2. The curves stack-up according to the increasing fluxoid numbers as: $k_zR = 0.5$; (0.5); 2.0.

3.2. Metallic cladding

When a superconductor is plated with a normal metal, the wave function is no longer constant at the interface but is instead systematically depressed. The extent of the depression is such that the slope of the wave function at the surface can be extrapolated to the value, ψ/δ, where the doping-controlled parameter δ is the extrapolation length. The condition of a zero gradient at the boundary is then modified according to [18]:

$$\frac{d\psi}{d\rho} + \frac{\psi}{\delta} = 0. \tag{15}$$

Fig. 4 shows the ϵ–f curves for the system of a solid cylinder in an azimuthal magnetic field plated with a normal metal. Each curve corresponds to a

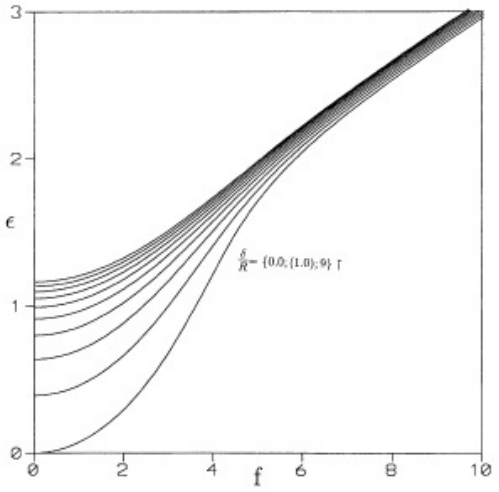

Fig. 4. The critical temperature versus the azimuthal critical field curves of a solid cylinder in a non-superconducting metallic matrix. The intercepts increase according to the values of the extrapolation length such that $R/\delta = 0.0$ for the lowest curve, increasing in unit steps up to $R/\delta = 9.0$ for the highest curve.

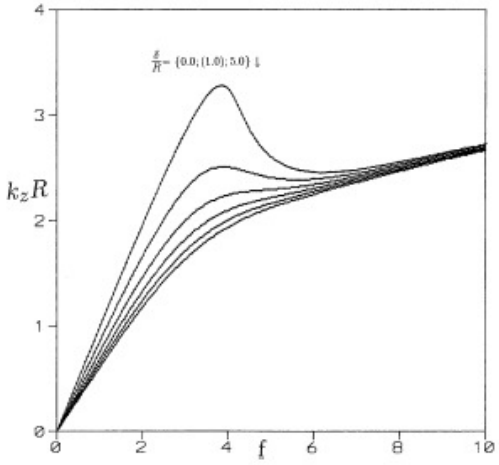

Fig. 5. The fluxoid eigenvalues as functions of the azimuthal critical field of a solid cylinder in a non-superconducting metallic matrix. The curves stack-up according to the decreasing values of the extrapolation length. The values of R/δ at $f = 4.0$, say, are 0.0 for the highest curve, increasing in steps of 0.5 up to 2.0 for the lowest curve.

different value of the extrapolation length. Going up the temperature axis along $f = 0$ the values of the extrapolation lengths are such that $R/\delta = 0.0$ for the lowest curve, increasing in unit steps up to 9.0 for the highest curve. The intercepts show a variation of the critical temperature with R/δ for zero magnetic field, in exact agreement with the results obtained by Masale et al. [6] and by Takács [7]. These graphs show an overall decrease of the critical temperature with an increase of R/δ, which is more pronounced for smaller values of the extrapolation length. The effect of metallic cladding can also be seen in the relation of the flux-entry points with the field, shown in Fig. 5. The value of R/δ varies from $R/\delta = 0.0$ for the highest curve and increases in steps of 0.5 for the more depressed curves, going down the k_zR axis, up to $R/\delta = 2.0$ for the lowest curve. The extent of the suppression of superconductivity increases with the decrease of the extrapolation length. This is accompanied by a decrease of the flux-entry points as the applied field is increased. This behaviour is typical of the other systems referred to in the text, namely a cylinder or a thin film in a parallel applied magnetic field. The curves corresponding to small values of R/δ in Fig. 5 show prominent peaks as a function of the field. These peaks, in fact, occur at the points of inflection on the ϵ–f curves and are rapidly smoothed out as R/δ increases. A similar behaviour, namely the quenching of the Little–Parks oscillations when R/δ is increased, has been noted for a thin-walled hollow cylinder in a parallel magnetic field [6].

4. Current-carrying cylindrical shell

The system considered here is a cylindrical shell of inner and outer surfaces bounded by R_1 and R_2, respectively. The current-induced magnetic field inside the shell may be written as follows:

$$B(\varphi) = \gamma \frac{B_s}{R_2}(\rho - R_1^2/\rho), \tag{16}$$

where $\gamma = 1/(1-\eta)$ in which $\eta = R_1^2/R_2^2$, which may be regarded as an index of the shell thickness. The vector potential associated with the magnetic field in Eq. (16) is given by:

$$A_z = -\gamma \frac{B_s}{R_2}\left[\frac{\rho^2}{2} - R_1^2 \ln(\rho/R_i)\right], \quad i = 1 \text{ or } 2. \tag{17}$$

For very fine filaments, of thicknesses much smaller that the G–L coherence length, there can hardly be spatial variations of the order parameter. In that case, the constant ψ approximate result is adequate for the determination of the critical field [19]. In fact, in the case of a very thin-walled hollow cylinder in a parallel magnetic field, the approximate and the full numerical results were found to be in exact agreement [6]. The form of the magnetic field given by Eq. (16) is bound to be fairly constant across the thickness of a very thin cylindrical shell. In view of this, any spatial variations of ψ that may arise as a result of changes of the superconducting phases across the shell thickness may be neglected. The constant ψ limiting form of the temperature is obtained on integrating the G–L equation across the shell thickness as follows:

$$\int_\eta^1 2\mu \frac{|\alpha|}{\hbar^2}\,\mathrm{d}x = \int_\eta^1 (|k_z| - 2\frac{e}{\hbar}A_z)^2\,\mathrm{d}x. \tag{18}$$

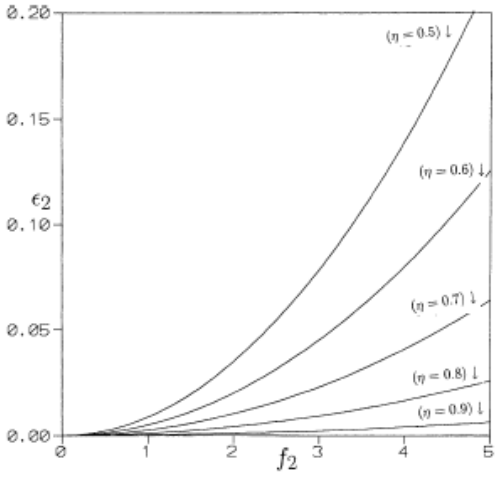

Fig. 6. The ϵ_2–f_2 curves of a current-carrying cylindrical shell. Each curve corresponds to a different thickness of the shell indicated there as values of $\eta = R_1^2/R_2^2$. The shell thicknesses, for example at $f = 5.0$, are such that $\eta = 0.9$ for the lowest curve, decreasing in steps of 0.1 down to 0.5 for the topmost curve.

Carrying out the integration, the limiting form of the temperature–field relationship is found as:

$$\epsilon_2 = \tfrac{1}{4}k_z^2 R_2^2 + \tfrac{1}{2}\gamma|k_z|R_2\left[1 + 3\eta + 2\eta^2\gamma \ln\eta\right]f_2 + \left[\tfrac{1}{3} + \tfrac{1}{2}\eta(3+5\eta)\gamma^2 + \eta^3\gamma^3 \ln\eta\left(3 - \tfrac{1}{2}\ln\eta\right)\right]f_2^2. \tag{19}$$

where the subscripts on ϵ and f indicate scaling of the definitions of the temperature and the field given by Eq. (8) in terms of R_2. Fig. 6 shows the ϵ_2–f_2 curves of thin-walled hollow cylinders of slightly different thicknesses. In Fig. 6 $\eta = 0.5$ for the highest curve, increasing in steps of 0.1 up to 0.9 for the lowest curves. It is clear from Fig. 6 that the critical field is significantly enhanced as a result of decreasing the thickness of the superconducting cylindrical shell.

5. Current-carrying core enveloped by a cylindrical shell

An idealized system might be a minute superconducting current-carrying core of radius R_1 and of a judiciously higher critical temperature than that of the superconducting cylindrical shell which envelopes it. In principle, therefore, the cylindrical shell should reach the field-induced transition to the normal state at lower fields than the core. A current inside the core generates a magnetic field whose vector potential in the region $\rho > R_1$ may be written as:

$$A_z = -\tfrac{1}{2}B_s R_2[1 + 2\ln(\rho/R_i)], \quad i = 1 \text{ or } 2. \tag{20}$$

Following the same analysis as for the system discussed in Section 4, the limiting form of the critical temperature as a function of the critical azimuthal field is found to be:

$$\epsilon_2 = \tfrac{1}{4}k_z^2 R_2^2 + [\gamma|k_z|R_2\eta \ln\eta]f_2 + [1 - \eta\gamma \ln^2\eta]f_2^2. \tag{21}$$

In deriving Eq. (21), although not necessary a priori, it was again assumed that the magnetic field is fairly uniform across the thickness of the very thin shell.

The field–temperature curves for this system are shown in Fig. 7 for the same parameters as for Fig. 6. The results here show a very similar behaviour

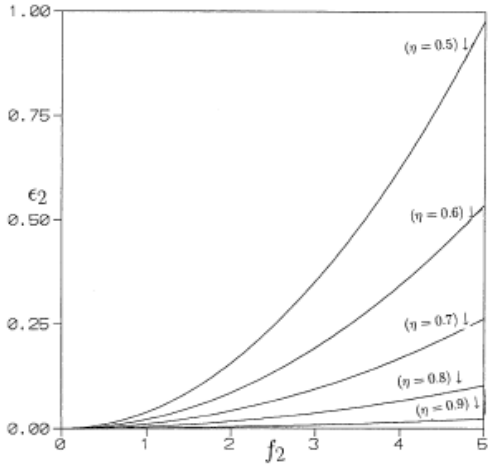

Fig. 7. The same caption as for Fig. 6 except that this is for a cylindrical shell cladding a current-carrying core.

as those of a current-carrying shell. It is seen from a comparison of Figs. 6 and 7 that, for the same thickness, the critical field for this system is significantly lower than that for the current-carrying shell for the same given critical temperature. This may be anticipated on realizing that the induced magnetic field increases with the increase in radial distance in the case of a current-carrying shell while the reverse is true in the case of a current-carrying core cladded with a thin metal sheet. To reach the critical field near R_2 of the shell cladded core a larger current is needed. Only the surface bounded by R_2 is at a further distance from the core and the field there is relatively weak.

6. Conclusions

The linearized G–L equation for the order parameter is solved to obtain the azimuthal critical field of some specific type II superconducting systems in form of cylindrical filaments. The applied magnetic field is thought to be generated by passing a current along the axis of the superconducting wire. In the thought experiment, the current is increased until it generates a magnetic field large enough to induce the transition from the superconducting state to the normal state. The surface nucleation field $H_{c3}(\phi)$, needed to induce this transition, has been calculated for the following systems: (a) free-standing solid cylinder, (b) solid cylinder in a non-superconducting metallic matrix, (c) current-carrying thin-walled hollow cylinder and (d) cylindrical shell cladding a current-carrying core. It is worth noting that the results of the investigations carried out are very similar to those obtained for the "reverse" problem for which the full G–L equation was employed [12]. For the same geometrical structures, the results point to a significantly higher critical azimuthal field compared to the parallel critical field. The results of this study point towards configurations which may have substantial advantages in the generation of high magnetic fields, for example, in superconducting electromagnets. Verification of these results should be possible in conventional experiments such as those of resistivity measurements or with the newly developed micro-magnetization measurement technique [17]. No specific conclusions can be drawn from these results about high-T_c superconductors in applied magnetic fields because only isotropic materials are considered. With the versatility of present-day experimental techniques, it may be worthwhile extending the discussed investigations to high-T_c materials.

References

[1] W. Meissner, R. Ochsenfeld, Naturwissenschaften 21 (1933) 787.
[2] S. Gygax, R.H. Kropschot, Phys. Lett. 9 (1964) 91.
[3] D. Saint-James, P.G. de Gennes, Phys. Lett. 7 (1963) 306.
[4] E. Guyon, F. Meunier, R.S. Thompson, Phys. Rev. 156 (1967) 452.
[5] S. Jin, J.E. Graebner, Mater. Sci. Eng. B 7 (1991) 243.
[6] M. Masale, N.C. Constantinou, D.R. Tilley, Supercond. Sci. Technol. 6 (1993) 287.
[7] S. Takács Czech, J. Phys. 19 (1969) 1366.
[8] N.C Constantinou, M. Masale, D.R. Tilley, J. Phys. C.: Condens. Matter 4 (1992) L293.
[9] W.A. Little, R.D. Parks, Phys. Rev. Lett. 9 (1962) 9.
[10] D.R. Tilley, J. Tilley, Superfluidity and superconductivity, Hilger, Bristol, 1990.
[11] H.J. Fink, L.J. Barnes, Phys. Rev. Lett. 15 (1965) 792.
[12] H.J. Fink, A.G. Presson, Phys. Rev. 151 (1966) 219.
[13] L.J. Barnes, H.J. Fink, Phys. Rev. 149 (1966) 186.

[14] R. Haslinger, R. Joynt, Phys. Rev. B 61 (2000) 4206.
[15] V.M. Fomin, V.R. Misko, J.T. Devreese, V.V. Moshchalkov, P.A. Maksym, Physica B 249–251 (1998) 476.
[16] C. Strunk, V. Bruyndoncx, C. Van Haesendonck, V.V. Moshchalkov, Y. Bruynseraede, C.J. Chien, B. Burk, V. Chrasekhar, Phys. Rev. B 57 (1998) 10854.
[17] A.K. Geim, I.V. Grigorieva, J.G.S. Lok, J.C. Maan, S.V. Dubonos, X.Q. Li, F.M. Peeters, Yu.V. Nazarov, Superlatt. Microstruct. 23 (1998) 151.
[18] P.G. de Gennes, Superconductivity of metals and alloys, Benjamin, New York, 1966.
[19] H.J. Fink, V. Grünfekl, Phys. Rev. B 22 (1980) 2289.